



Technical note: Reactive transport modelling -a technique to understand coupled chemical processes in porous media

Soumaia M'nassri^{1*}, Rajouene Majdoub¹

¹*Laboratory of Research in Management and Control of Animal and Environmental Resources in Semi-arid Ecosystem,
Higher Agronomic Institute of Chott Meriem, University of Sousse, BP 42, 4042, Tunisia*

*Corresponding author, Email address: mnassrisoumaia@gmail.com

Received 10 Apr 2022,
Revised 04 May 2022,
Accepted 05 May 2022

Keywords

- ✓ Reactive and transport modelling,
- ✓ Dissolved species,
- ✓ Chemical processes,
- ✓ Porous Media
- ✓ KIRMAT model.

mnassrisoumaia@gmail.com

Abstract

We present a reactive transport model that has proven to be an invaluable tool for modeling soluble salt transport processes at temporal and spatial scales in porous media. Quantifying salt changes and predicting their future behavior are critical for reducing the risks of water and soil degradation and, as a result, taking the necessary measures for rational water resource management and long-term development of the study regions. It begins with the conceptualization and discretization of the model section. For each zone outlined in the modelled domain, the mineralogical compositions, reactive surface, thermodynamic, kinetic, and hydrodynamic parameters are then calculated. In addition, we identified the simulation's initial and boundary conditions, as well as the simulation's covering period. The findings show the effectiveness of the Kinetic Reaction and Mass Transport code (KIRMAT), which could be used to predict chemical species. Reactive transport modeling has proven to be a successful method for simulating complex natural systems. It is applicable to a wide range of geoscientific problems.

1. Introduction

Water scarcity is among the most significant threats facing the world, and the Mediterranean regions in general, on all thresholds: socioeconomic, financial, governmental, and ecologic. Water scarcity becomes more acute when it is combined with the degradation of its quality, most notably by the phenomenon of salinization [1, 2].

Numerous investigations on the issue of salinization have been carried out [3, 4, 5]. Even so, due to its complexity, there is still a substantial uncertainty about the prediction and evolution of salinization of water and soil resources in the medium and long term. Indeed, salinization of water resources is caused by a multitude of processes, including water and solute transfer processes as well as geochemical processes [6,7]. Although each of these processes has been studied extensively on its own, the understanding of their interactions is still limited. Furthermore, the aquifer's mass fluxes and chemical composition can shift radically over time and space. Hence, one method for overcoming these issues is to use numerical modelling [8, 9].

Historically, a large number of geochemical efforts have been made. In these, equilibrium-based models use the local equilibrium assumption, which presumes that all chemical reactions will complete or reach equilibrium within each time step [10]. However, kinetic methods enable you to recognize the rates of all chemical reactions occurring [11]. The most advanced tools are reactive transport models. They can be used to estimate geochemical processes as well as dissolved species' future behavior [12].

The text is organized as follows: section 2 presents the mathematical formulation of reactive transport models; Section 3 describes the used method, including all steps of modeling approach as well as the input data. The results and discussion are presented in section 4. The summary is in the fourth section.

2. Mathematical formulations of reactive-transport models

The geochemical models of reactive transport are based on thermodynamic and kinetic concepts, which are combined with the mass transport effect that occurs within the system [13]. Indeed, numerous geochemical models developed in the literature are based on thermodynamic equilibrium relationships that require defining the state of evolution of an assembly composed of soil or rock and a solution. The law of mass action determines equilibrium relationships [14]. It is given by Eq .1.

$$K_T = \frac{\{C\}^{v_C} \{D\}^{v_D}}{\{A\}^{v_A} \{B\}^{v_B}} \quad \text{Eq.1}$$

Where K_T : equilibrium constant, A, B, C and D: chemical species and v_A , v_B , v_C and v_D : stoichiometric coefficients of the reaction.

The activity coefficient in Eq.1 is determinate by the interactions that exist between the various dissolved molecules in solution. As a result, in the case of a very dilute solution, the activity coefficient equals 1. For ionic strengths (I) less than 0.2 mol L^{-1} , the activity coefficients are calculated using the [15] model, as shown in Equation 2.

$$\log \alpha_i = - \frac{AZ_e^2 \sqrt{I}}{1 + a_e B \sqrt{I}} + C I \quad \text{Eq.2}$$

Where A and B are the solvent's characteristic constants, Z is the charge of the ion e, C is the ion's concentration, and a_e is its ionic activity.

Additionally, the ionic product (Q_T), defined by equation 3, is also another thermodynamic quantity characteristic of the evolution state of the chemical reaction.

$$Q_T = \frac{\{C\}^{v_C} \{D\}^{v_D}}{\{A\}^{v_A} \{B\}^{v_B}} \quad \text{Eq.3}$$

The estimation of the ratio between the equilibrium constant and the ionic product reflects a solution's saturation, under saturation, and equilibrium towards a mineral. If the water sample is completely saturated with the dissolved mineral, SI equals zero. Positive values of SI indicate supersaturation under which the mineral would tend to precipitate; negative values indicate undersaturation and mineral dissolution. The above-mentioned thermodynamic quantities make it possible to determine the evolution of geochemical processes. However, they could not provide any information about their dynamics. As a result, kinetic characterization of the various reactions occurring within the soil or water table is critical. Several studies have been conducted on the kinetics of calcites, carbonates, and evaporates [16]. The kinetics of mineral dissolution and precipitation reactions, as expressed by equations 4 and 5, are the primary focus of these works.

$$V_d = k_d S_{ref}^{eff} a_{H+}^{n_r} \left[1 - \frac{Q_T}{K_T} \right] \quad \text{Eq.4}$$

Where V_d : dissolution rate of the mineral ($\text{mol yr}^{-1} \text{ kg}^{-1} \text{ H}_2\text{O}$), k_d : intrinsic dissolution constant ($\text{mol m}^{-2} \text{ yr}^{-1}$), S_{ref} : reactive surface of the mineral in contact with one kilogram of solution (m^2

$\text{kg}^{-1}\text{H}_2\text{O}$), $a\text{nH}^+$: activity of the H^+ ion in solution and n_r : partial order of the reaction with respect to the H^+ ion in solution.

$$V_p = k_p S_r^{\text{eff}} \left(\left(\frac{\varrho_r}{K_r} \right)^p - 1 \right)^q \quad \text{Eq. 5}$$

Where V_p denotes the mineral's precipitation rate ($\text{mol yr}^{-1} \text{kg}^{-1}\text{H}_2\text{O}$), k_p the intrinsic precipitation constant ($\text{mol m}^{-2} \text{yr}^{-1}$), and p and q the experimentally determined exponents describing the mineral's precipitation rate in the oversaturated state.

Several studies have been conducted to estimate the reactive surface of the minerals reacting with the solution in the various kinetic formalisms. Some researchers used the Brunauer-Emmet-Teller method to physically measure the reactive surface, while others quantified it numerically such as [17]. They computed the reactive surface area from the geometry and particle arrangement expressed by Equation. 6, and from the volume fraction and porosity expressed by Equation 7.

$$S_r^{\text{eff } n} = S_r^{\text{eff } n-1} \left(\frac{1-\omega^n}{1-\omega^{n-1}} \right)^{2/3} \quad \text{Eq. 6}$$

$$S_r^{\text{eff } n} = S_r^{\text{eff } n-1} \left(\frac{\omega^{n-1}}{\omega^n} \right) \left(\frac{Fv^n}{Fv^{n-1}} \right)^{2/3} \quad \text{Eq. 7}$$

Where S_r^{eff} is the reactive surface area of a mineral, r , n , and $n-1$ are the time increments, ω : porosity, and Fv is the mineral's volume fraction.

The three main mechanisms of dissolved chemical species migration in water are advection, kinematic dispersion, and molecular diffusion. The mass conservation equation for a reactive element (j) in a one-dimensional system makes it possible to create the model that governs its transport (Eq. 8).

$$\frac{\partial}{\partial t} (\omega \Psi_j) = -V \frac{\partial \Psi_j}{\partial x} + \omega D^* \left(\frac{\partial^2 \Psi_j}{\partial x^2} \right) - \sum_{r=1}^M v_{jr} \frac{\partial}{\partial t} (F_v V_r) \quad \text{Eq. 8}$$

Where Ψ_j : generalized concentration of element j ($j=1, \dots, N$), t : transport time (yr), V : Darcy velocity (m yr^{-1}), D^* : hydrodynamic dispersion coefficient, M : primary species of reactive minerals, and V_r : molar volume of mineral.

3. Methodology

Using the reactive-transport modeling method with the Kinetic Reaction and Mass Transport model (KIRMAT) entails a number of steps and decisions: First, an appropriate construction and discretization scheme is selected. The modelled section can be chosen according to the groundwater flow directions. Then, it must be critiqued with horizontal meshes spacing of 300 m-long meshes that allow for a more accurate description of the shape of the study area. Following that, the modelled domain is divided into zones based on the number of wells located along the conceptualized domain. The initial and boundary conditions are then defined. In fact, the model's initial condition is based on the average chemical composition of all observed wells along each modelled section. The concentration of the upstream boundary is used as a fixed-concentration corresponding to a 1st or type, or Dirichlet boundary. The prescribed concentrations are based on the measured concentrations of the first observation well located upstream of the modelled section. The downstream boundary has been designated as a free flux boundary. Furthermore, the mineralogical compositions and reactive surfaces

of the minerals are identified for each zone of the modelled section. S_{eff}, the reactive surface, is calculated as follows:

$$S_r^{eff} = V_m \frac{S_{cube}}{V_{cube}} \quad \text{Eq.9}$$

Where V_m: volume of mineral per kilogram of water (m³ kg⁻¹), S_{cube} and V_{cube}: area (m²) and volume (m³) of the cube, respectively. V_m is calculated as follows

$$V_m = F_v \frac{(1-\omega)*1000/\rho}{\omega} \quad \text{Eq. 10}$$

Where F_v: volume fraction of mineral, ω: porosity, ρ: density of water (kg m⁻³).

The hydrodynamic, thermodynamic and kinetic data are also used as input parameters in the KIRMAT model. The hydrodynamic parameters used are hydraulic conductivity (K), Darcy velocity (U), total porosity (ρ) and effective porosity (η). For the thermodynamic constants for each mineral, they are obtained from the KIRMAT code's MIN.Dat data. The temperature chosen can be determined by the average temperature recorded in the various points of water taken from the groundwater. Equation 11 is used to calculate the kinetic dissolution rate of the minerals taken into account.

$$V_d = S_r^{eff} \left(1 - \frac{Q_T}{K_T} \right) \begin{bmatrix} k_{25}^{Acid} \exp \left[\frac{-E_a^{Acid}}{R} \left(\frac{1}{T} - \frac{1}{298,15} \right) \right] \alpha_{Acid}^{nAcid} \\ + k_{25}^{Neutre} \exp \left[\frac{-E_a^{Neutre}}{R} \left(\frac{1}{T} - \frac{1}{288,15} \right) \right] \\ + k_{25}^{Base} \exp \left[\frac{-E_a^{Base}}{R} \left(\frac{1}{T} - \frac{1}{298,15} \right) \right] \alpha_{Base}^{nBase} \end{bmatrix} \quad \text{Eq.11}$$

Where V_d: dissolution rate controlled by the reactive surface (mol yr⁻¹ kg⁻¹H₂O), k₂₅^{acid}, k₂₅^{neutral}, k₂₅^{base}: dissolution constants at 25°C; S_r^{eff}: reactive surface of the minerals, Q_T: ionic activity product, K_T: thermodynamic equilibrium constant, E_a^{acid}, E_a^{neutre}, E_a^{base}: activation energy coefficients (J mol⁻¹); n_{acid} and n_{base}: orders of the chemical reaction and R is the perfect gas constant (J K⁻¹ mol⁻¹) at temperature T (°C).

Finally, the model must be calibrated and validated. Statistical indices such as the root-mean-square-error (RMSE) between computed and observed concentrations of each monitoring point is used to assess the model's response (Eq. 12).

$$\text{RMSE} = \sqrt{\frac{1}{n} \sum (O_i - C_i)^2} \quad \text{Eq.12}$$

Where O_i: measured values of the concentration C of the element i, C_i: calculated values of the concentration C of the element i in solution, and n: number of observations.

4. Results and Discussion

4.1 Application to predict chemical species in groundwater (50 and 100-years)

Figure 1 depicts spatial and temporal changes in the dominant chemical elements in solution. Two time steps are used to simulate chemical concentrations (50 years, and 100 years). The spatial analysis of the different chemical profiles reveals an increase in chloride and sodium concentrations throughout T1.

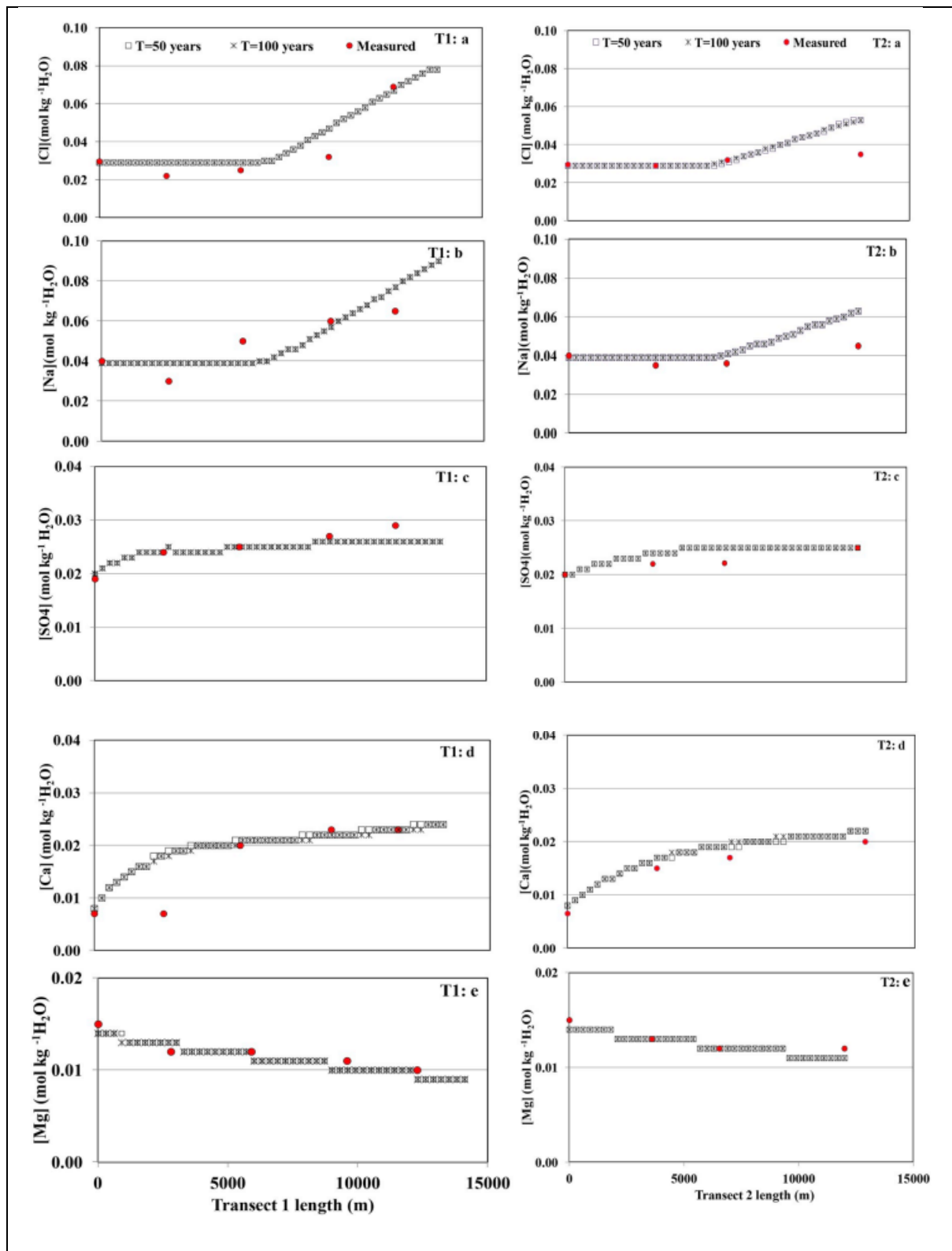


Figure 1. Spatiotemporal evolution of chemical species along transects T1 and T2: (a) chlorides, (b) sodium, (c) sulphates, (d) calcium, and (e) magnesium.

The levels of the latter chemical elements measured at the transect's end are in the order of $0.08 \text{ mol kg}^{-1} \text{ H}_2\text{O}$ and $0.09 \text{ mol kg}^{-1} \text{ H}_2\text{O}$, respectively. The shape of the chloride and sodium curves in transect 2 is similar to that observed in transect 1, but with lower contents due to halite deficiency in zones 1 and 2.

The predominance of halite (NaCl) dissolution kinetics over precipitation explains the gradual increase in chloride and sodium levels in the water table. After 100 years of changes, a slight decrease in Cl^- and Na^+ content was observed at $x=6000$ m, indicating a decrease in halite mass and, as a result, a decrease in the reactive surface of this mineral during the dissolution process [18]. Increased Cl and Na concentrations are found primarily in cells which contain the minerals halite. As a result, the contact between halite and groundwater has a significant impact on the spatiotemporal evolution of dissolved sodium and chloride.

As for the chemical profiles of sulfates, the concentrations are globally constant with an increasing trend, particularly in the last zones of transects T1 and T2 with a content of about $0.02 \text{ mol Kg}^{-1}\text{H}_2\text{O}$. At 100 years of alteration, the sulphate profile shows a similar evolution to that observed at 50 years resulting from the competition between the processes of dissolution and precipitation of sulphate minerals, namely gypsum and anhydrite. Calcium concentrations are gradually increasing until they reach $0.02 \text{ mol Kg}^{-1} \text{ H}_2\text{O}$. From the distance $x=7000$ m, both profiles show stable calcium contents. The calculated SO_4 and Ca concentrations rise as one travels further. The dissolution of gypsum and anhydrite is the most logical source of these ions.

In contrast to the previously mentioned chemical elements, the magnesium profiles show a decrease across transects 1 and 2 on the one hand, and over time on the other. This decrease could be explained by the contribution of these ions to calcite and/or dolomite precipitation.

4.2 Calibration and validation of model

Different numerical runs are performed to adjust the model. The best fit of the measured chemical compositions is obtained for the adjusted dissolution rates. The model provides a good estimate of chemical elements for the two modelled transects T1 and T2 with a RMSE value of approximately 0.01 for all of the chemical species. The numerical results were close to the field data. The obtained correlation coefficients show an acceptable correlation between measured and simulated chemical concentrations for T1 and T2 (Fig. 2).

The model's sensitivity is investigated in three cases: i) variation of the volume fraction of minerals up to 10%, ii) variation of the chemical compositions of the injected flows using the chemical concentrations of the first water point located upstream of the transect, and iii) variation of the Darcy velocity. The results show that the model is rather sensitive to the volume fraction variation. However, the chemical composition and the Darcy velocity are not sensitive model parameters.

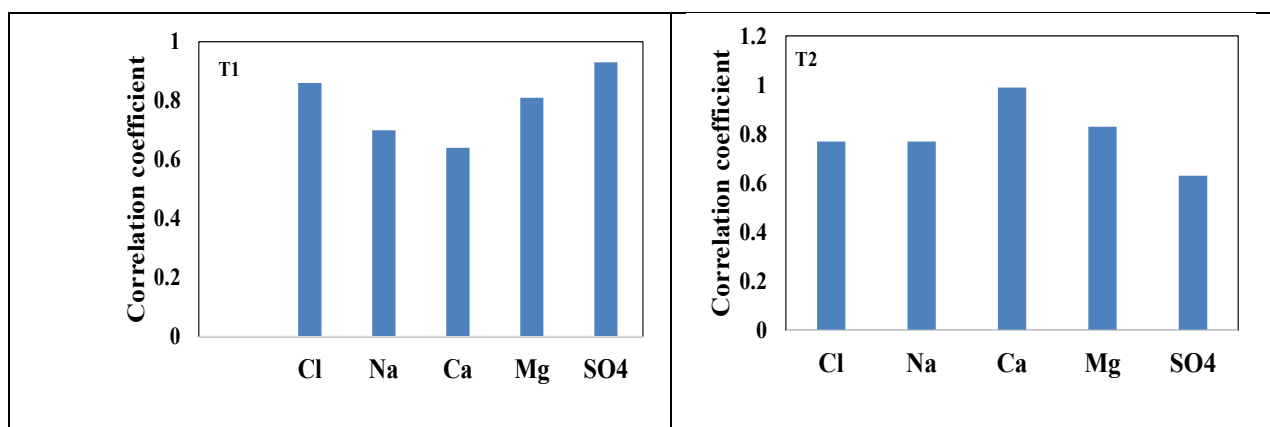


Figure 2. Correlation coefficient of chemical species between measured and computed values

Conclusion

In this paper, we present a reactive transport model for simulating groundwater chemical species in order to find suitable management scenarios for deteriorated aquifers. The model was successfully calibrated and validated. It is only sensitive to the volume fraction of the minerals considered. We also recommend using this method in a saturated zone.

Acknowledgement

We would like to express our gratitude to Lucas Yann and Gerhard Schafer for providing the KIRMAT code.

Data availability: All data used in the reactive transport modeling, as well as the detailed results, are publicly available at <https://doi.org/10.1016/j.apgeochem.2019.01.018>.

Disclosure statement: *Conflict of Interest:* The authors declare that there are no conflicts of interest.

Compliance with Ethical Standards: This article does not contain any studies involving human or animal subjects.

References

- [1]. R.T. Bailey, J. Jaehak, S. Park, H.M. Green, “Simulating salinity transport in High-Desert landscapes using APEX-MODFLOW-Salt”, “*Journal of Hydrology*, 610 (2022) 127873.
- [2]. S. M’nassri, L. Dridi, Y. Lucas, G. Schäfer, M. Hachicha and R. Majdoub, “Identifying the origin of groundwater salinisation in the Sidi El Hani basin in central-eastern, Tunisia”, “*Journal of African Earth Sciences*, 147 (2018) 443–449.
- [3]. A. Singh, “Environmental problems of salinization and poor drainage in arrigated areas: Management through the mathematicak models”, “*Journal of Cleaner Production*, 206 (2019) 572-579.
- [4]. J.V. Gend, M.L. Francis, A.P. Waston, L. Palcsu, A. Horvath, P.H. Macey, P. Le. Roux, C.E. Clarke, J.A. Miller, “Saline groundwater in the Buffels river catchment, Namaqualand, South Africa: A new look at an old Problem”, “*Science of the Total Environment*, 762 (2021) 143140.
- [5]. S. M’nassri, L. Dridi, G. Schäfer, M. Hachicha and R. Majdoub, “Groundwater salinity in a semi-arid region of central-eastern Tunisia: insights from multivariate statistical techniques and geostatistical modelling”, “*Environmental Earth Sciences Journal*, 78(2019a) 288.
- [6]. A. Jenni, C.L. Meeussen, T.A. Pakkanen, J. Vizcaino, E. Muuri, M. Niskanen, P. Wersin, U. Mader, “Coupling of chemical and hydrochemechanical properties in bentonite: A new reactive transport model”, “*Applied Clay Science*, 214 (2021) 106247.
- [7]. M. Pieretti, T. Karlsson, S. Arvilommi, M. Muniruzzaman, Challenges in predicting the reactive of mine waste rocks based on kinetic testing: humidity cell tests and reactive transport modeling”, “*Journal of Geochemical Exploration*, 237 (2022) 106996.
- [8]. R. Lu, T. Nagel, J. Poonoosamy, D. Naumov, Th. Fisher, V. Montya, O. Kolditz, H. Shao, “Anew operator-splitting finite element scheme for reactive transport modelling in saturated porous media”, “*Computers and Geosciences*, 163 (2022) 105106.
- [9]. S. M’nassri, Y. Lucas, G. Schäfer, L. Dridi and R. Majdoub, “Coupled hydrogeochemical modelling using KIRMAT to assess water-rock interaction in a saline aquifer in central-eastern Tunisia”, *Applied Geochemistry Journal*, 102 (2019b) 229-242.

- [10]. H.S. Gatz-Miller, F. Gerard, E.P. Verrecchia, S. Danyang, K.U. Mayer, “reactive transport modelling the oxalate-carbonate pathway of the Iroke tree: Investigation of calcium and carbon sinks and sources”, “*Geoderma*, 410 (2022) 115665.
- [11]. J.M. Abril, H. Barros, “Modelling the kinetic reactive transport of pollutants at the sediment-waste interface. Applications with atmospheric fallout radionuclides”, “*Journal of Environmental Radioactivity*, 242 (2022) 106790.
- [12]. N. Seigneur, B. Vriens, R.D. Beckie, K.U. Mayer, “Reactive transport modelling to investigate multi-scale waste rock weathering processes”, “*Journal of Contaminant Hydrology*, 236 (2021) 103752.
- [13]. D. Roubinet, Ph. Gouze, A. Puyguiraud, M. Dentz, “Multi-scale random walk models for reactive transport processes in fracture-matrix system”, “*Advances in Water Resources*, 164 (2022) 104183.
- [14]. R.H. Deucher, H.A. Tchelepi, “Adaptive formulation for two-phase reactive transport in heterogenous porous media”, “*Advances in Water Resources*, 155 (2021) 103988.
- [15]. J. Soler-Sagarra, M. W. Saaltink, A. Nardi, F. De Gaspari, J. Carrera, “Water mixing approach (WMA) for reactive transport modelling”, “*Advances in Water Resources*, 161(2022) 104131.
- [16]. H. Deng, J. Poonoosamy, S. Molins, “A reactive transport modelling perspective on the dynamics of interface-coupled dissolution-precipitation”, “*Applied Geochemistry*, 137 (2022) 105207.
- [17]. A. Iraola, P. Trinchero, S. Karra, J. Molinero, “Assessing dual continuum method for multicomponent reactive transport”, “*Computers and Geosciences*, 130 (2019) 11-19.
- [18]. D. Prikryl, A. Jha, S. Stefansson, S.L. Stipp, “Mineral dissolution in porous media: An experimental and modeling study kinetics, porosity and surface area evolution”, “*Applied geochemistry Journal*. 87 (2017) 57-70.

(2022) ; <http://www.jmaterenvironsci.com>